Jakub Cieśluk, Zdzisław Gosiewski, Leszek Ambroziak, Sławomir Romaniuk
Computationaly Simple Obstacle Avoidance Control Law for Small Unmanned Aerial Vehicles

DOI 10.1515/ama-2015-0010

COMPUTATIONALY SIMPLE OBSTACLE AVOIDANCE CONTROL LAW
FOR SMALL UNMANNED AERIAL VEHICLES

Jakub CIEŚLUK*, Zdzisław GOSIEWSKI*, Leszek AMBROZIAK*, Sławomir ROMANIUK*

*Faculty of Mechanical Engineering, Automatic Control and Robotics Department, Bialystok University of Technology,
ul. Wiejska 45C, 15-351 Białystok, Poland

jakub_ciesluk@wp.pl, z.gosiewski@pb.edu.pl, l.ambroziak@pb.edu.pl, s.romaniuk@doktoranci.pb.edu.pl

Abstract: The investigations of the system which allow to avoid obstacles by the unmanned aerial vehicles (UAV) are presented in the paper. The system is designed to enable the full autonomous UAV flight in an unknown environment. As an information source about obstacles digital camera was used. Developed algorithm uses the existing relations between the imaging system and the parameters read from the UAV autopilot. Synthesis of the proposed obstacle avoidance control law was oriented for computational simplicity. Presented algorithm was checked during simulation studies and in-flight tests.

Key words: Unmanned Aerial Vehicle, Quadrotor Control, Obstacle Avoidance, Vision Systems

1. INTRODUCTION

Unmanned Aerial Vehicles (UAVs) have wide range of applications - military and civil. Although they are able to perform a part or even the whole mission automatically, do not have the full autonomy. Autonomy level can be increased in substantial way by means of obstacle avoidance systems.

In the past, graph methods (Shojaeopour, 2010) and potential fields (Khatib, 1985) approach were utilized to the path planning in autonomous navigation. Nowadays UAVs obstacle avoidance problems are mainly resolved by the usage of fuzzy logic (Cieśluk and Gosiewski, 2012, 2013; Guzel and Bicker, 2011) and methods of predictive control (Wang, 2001). Devices used as the obstacle detection sensors are ultrasonic range finders (Modi et al., 2001), laser scanners (Kownacki, 2013), lidars (Sabatini et al., 2014) and vision sensors (ccd cameras (Meier et al., 2012), optical flow sensors (Herrise et al., 2008)). Despite first three of mentioned sensors have fairly good range measurements quality, their mass is relatively large and they have low output frequency (Modi et al., 2001).

The following paper presents the obstacle avoidance control law based on the fuzzy logic controller. Input to the fuzzy logic controller is the information acquired from the cameras. Obtained information from vision system can be easily adopted to fuzzy logic rules. Proposed algorithm is based on a small number of input parameters, what results in low requirements of computational power. Main goal of the presented studies was simulation tests. During this tests preliminary process of the control surface selection was performed. Moreover presented control algorithm was checked during in-flight tests.

2. RESEARCH OBJECT

2.1. Quadrotor

As control object we have chosen quadrotor - vertical take-off and landing (VTOL) object with very specific dynamics. Quadrotors are often used as a platform for formation flying control framework, surveillance and reconnaissance purposes, aerial surveys for agriculture, traffic monitoring etc. They can hover above the desired waypoint and in place can change the motion direction. It is simple to separate navigation from orientation in quadrotor motion. Simplified dynamics model of this objects is described in the next subsection.

2.2. Mathematical model

Methods described in the work of authors (Cieśluk and Gosiewski, 2013; Soumare et al., 2002) allow obstacle detection in the robot's surroundings. However, in order to avoid an obstacle, location itself is insufficient. The adequate control procedure is required, which take into account data read from the obstacle localization sensor. Thus, in order to present the idea of control algorithm used in the obstacle avoidance flight mode, mathematical model employed in the quadrotor research is used.

Determination of the dynamic model of the quadrotor required linking together of the two coordinate systems. First coordinate system is associated with the object $-x_B, y_B, z_B$ while the other one is associated with the Earth $- x, y, z$ (Fig. 1). Quadrotor center of gravity is the origin of coordinate system x_B, y_B, z_B.
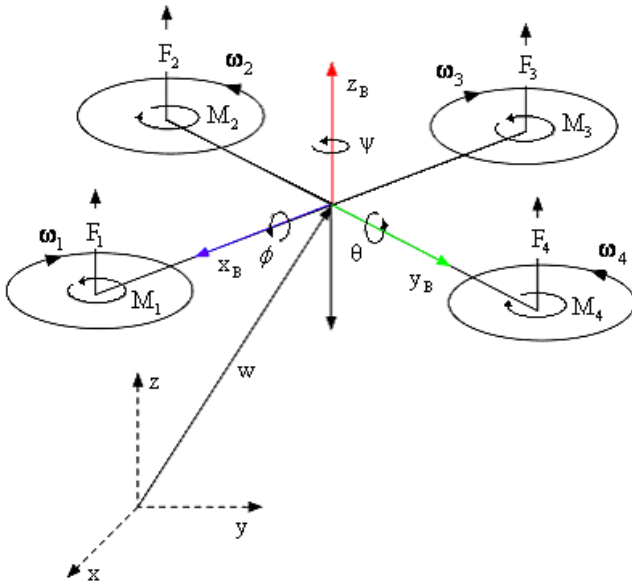
Fig. 1. Quadrotor coordinates frame

Description of the variables containing position and orientation data of the quadrotor in 3D space is described underneath:

$$\begin{bmatrix} x \\ y \\ z \end{bmatrix} = \begin{bmatrix} longitude \\ latitude \\ altitude \end{bmatrix}, \begin{bmatrix} \phi \\ \theta \\ \psi \end{bmatrix} = \begin{bmatrix} roll\ angle \\ pitch\ angle \\ yaw\ angle \end{bmatrix} \qquad (1)$$

Vector containing data of linear and angular quadrotor position related to Earth coordinate system $x, y,$ is specified as follows:

$$q = [x\ y\ z\ \phi\ \theta\varphi]^T \qquad (2)$$

Vector comprising linear velocities and angular rates components of quadrotor in the x_B, y_B, z_B system is defined below:

$$\dot{q_B} = [u\ v\ z\ p\ q\ r]^T \qquad (3)$$

Relations between two corresponding coordinate systems can be written in the following way based on Mellinger et al. (2012) and Hoffmann et al., (2011):

$$\begin{bmatrix} \dot{x} \\ \dot{y} \\ \dot{z} \end{bmatrix} = R_B \begin{bmatrix} u \\ v \\ n \end{bmatrix}$$
$$\triangleq \begin{bmatrix} c_\psi c_\theta & -s_\psi c_\phi + c_\phi s_\theta s_\phi & s_\psi s_\phi + c_\psi s_\theta c_\phi \\ s_\psi c_\theta & c_\psi c_\phi + s_\phi s_\theta s_\psi & -c_\psi s_\phi + s_\psi s_\theta c_\phi \\ -s_\theta & c_\theta s_\phi & c_\theta c_\phi \end{bmatrix} \begin{bmatrix} u \\ v \\ n \end{bmatrix}, \qquad (4)$$
$$\begin{bmatrix} \dot{\phi} \\ \dot{\theta} \\ \dot{\psi} \end{bmatrix} = T_B \begin{bmatrix} p \\ q \\ r \end{bmatrix} \triangleq \begin{bmatrix} 1 & s_\phi t_\theta & c_\phi t_\theta \\ 0 & c_\phi & -s_\phi \\ 0 & s_\phi/c_\theta & c_\phi/c_\theta \end{bmatrix} \begin{bmatrix} p \\ q \\ r \end{bmatrix}$$

$$\dot{q} = \begin{bmatrix} R_B & 0_{3\times3} \\ 0_{3\times3} & T_B \end{bmatrix} \dot{q_B},$$

where: c_θ, s_θ, t_θ are shortened notation of $\cos(\theta), \sin(\theta)$, $\tan(\theta)$, similarly for the remaining angles ϕ and ψ. Vector w in Fig. 1 describes the position of mass center in the global coordinate system. The gravitation force in the $-z$ direction and the motors thrust F_i in the z_b direction are the forces acting on the quadrotor. Equation presenting the acceleration of the mass center is described as follows:

$$m\ddot{w} = \begin{bmatrix} 0 \\ 0 \\ -mg \end{bmatrix} + R_B \begin{bmatrix} 0 \\ 0 \\ \sum F_i \end{bmatrix} \qquad (5)$$

Every motor generates torque M_i, that is parallel to the propellers rotation plane. Rotor 1 and 3 have clockwise direction of rotation while 2 and 4 have counterclockwise direction. Motor torques have directions opposing to the propellers rotation one. Thus, M_1 and M_3 have $-z_b$ direction while M_2, M_4, z_b direction. The length of each of the quadrotor arms is l. Moment of inertia matrix related to the mass center along the $x_B y_B z_B$ axis is I. Angular acceleration described by Euler equation is following:

$$I \begin{bmatrix} \dot{p} \\ \dot{q} \\ \dot{r} \end{bmatrix} = \begin{bmatrix} l(F_4 - F_2) \\ l(F_3 - F_1) \\ -M_1 + M_2 - M_3 + M_4 \end{bmatrix} - \begin{bmatrix} p \\ q \\ r \end{bmatrix} \times I \begin{bmatrix} p \\ q \\ r \end{bmatrix} \qquad (6)$$

Having regard to the (5) and (6) quadrotor dynamic system equations are received:

$$\begin{cases} \ddot{x} = \left(s_\psi s_\phi + c_\psi s_\theta c_\phi \right) \frac{u_1}{m} \\ \ddot{y} = \left(-c_\psi s_\phi + s_\psi s_\theta c_\phi \right) \frac{u_1}{m} \\ \ddot{z} = -g + \left(c_\theta c_\phi \right) \frac{u_1}{m} \\ \dot{p} = \frac{I_{yy} - I_{zz}}{I_{xx}} qr + \frac{u_2}{I_{xx}} \\ \dot{q} = \frac{I_{zz} - I_{xx}}{I_{yy}} pr + \frac{u_3}{I_{yy}} \\ \dot{r} = \frac{I_{xx} - I_{yy}}{I_{zz}} pq + \frac{u_4}{I_{zz}} \end{cases} \qquad (7)$$

The description of system input variables u_i will be presented in the next section.

2.3. Orientation control

Linearization of the quadrotor equations of motion can be made in the properly chosen equilibrium point. Selected equilibrium point parameters are:

$w = w_0, \theta = \phi = 0,\ \psi = \psi_0,\ \dot{w} = 0, \dot{\phi} = \dot{\theta} = 0\ \dot{\psi} = 0.$

Taking assumption that roll and pitch angles of the system are very small we can write that:

$cos\phi \approx 1,\ cos\theta \approx 1,\ sin\phi \approx \phi,\ sin\theta \approx \theta.$

Nominal force generated by motor-propeller systems in a given state is defined as follows:

$$F_{i,0} = \frac{mg}{4} \qquad (8)$$

Presented model of the quadrotor is symmetrical, therefore $I_{xx} \approx I_{yy}$, so according to equation (6) we can write:

$$I_{xx}\dot{p} = u_2 - qr(I_{zz} - I_{yy})$$
$$I_{yy}\dot{q} = u_3 - pr(I_{xx} - I_{zz}) \qquad (9)$$
$$I_{zz}\dot{r} = u_4$$

Resultant torque values are determined by simple, proportional-differentiating control laws, presented below:

Jakub Cieśluk, Zdzisław Gosiewski, Leszek Ambroziak, Sławomir Romaniuk
Computationaly Simple Obstacle Avoidance Control Law for Small Unmanned Aerial Vehicles

DOI 10.1515/ama-2015-0010

$$u_{2,des} = k_{p,\phi}(\phi_{des} - \phi) + k_{d,\phi}(p_{des} - p)$$

$$u_{3,des} = k_{p,\theta}(\theta_{des} - \theta) + k_{d,\theta}(q_{des} - q) \qquad (10)$$

$$u_{4,des} = k_{p,\psi}(\psi_{des} - \psi) + k_{d,\psi}(r_{des} - r)$$

Each of the rotors during operation has a fixed angular velocity ω_i and a vertical force is generated in accordance with the following formula:

$$F_i = b\omega_i^2 \qquad (11)$$

while torque is determined by term:

$$M_i = d\omega_i^2 \qquad (12)$$

Important aerodynamic parameters describing the behavior of rotating propellers in the air are taken into account during the calculations. Those parameters are: $b\ [\mathrm{N/rpm^2}]$ which is an aerodynamic longitudinal coefficient (thrust) and $d\ [\mathrm{Nm/rpm^2}]$ describing air resistance coefficient of the rotating body. Designation of these aerodynamic parameters is done by combining the momentum theory and the theory of the propeller thoroughly described in Bresciani (2008) according to the relations:

$$b = \frac{T_{BET}}{\omega_i^2} \qquad (13)$$

$$d = \frac{Q_{BET}}{\omega_i^2} \qquad (14)$$

where: longitudinal force T_{BET} [N] is found by the integration of the vertical forces acting on all sections of the blade elements. Furthermore, the torque of the propeller Q_{BET} [Nm] is found by integrating the horizontal forces multiplied by the moment arm on all sections of the blade components.

Setpoint value of the motor angular speed is limited to the range from 1200rpm to 8000rpm. Preset speeds of the individual motors $\omega_{i,des}^2$, can be find from the set resultant force value's data $u_{1,des}$ and moments ($u_{2,des}$, $u_{3,des}$, $u_{4,des}$) by transforming following equation:

$$\begin{bmatrix} u_{1,des} \\ u_{2,des} \\ u_{3,des} \\ u_{4,des} \end{bmatrix} = \begin{bmatrix} b & b & b & b \\ 0 & -bl & 0 & bl \\ -bl & 0 & bl & 0 \\ -d & d & -d & d \end{bmatrix} \begin{bmatrix} \omega_{1,des}^2 \\ \omega_{2,des}^2 \\ \omega_{3,des}^2 \\ \omega_{4,des}^2 \end{bmatrix} \qquad (15)$$

2.4. Position control

To present the idea of the UAV position control, some simplifications were adopted. They result from taking into account the motion (lifting) of the quadrotor to (x, y, z_B) position. It is possible, consequently to assume that tracked yaw angle is $\psi_T(t) = \psi_0$.

The linearization of equation (5) allows us to establish the relation between specified linear acceleration, roll and pitch angles as follows:

$$\ddot{w}_{1,des} = (\phi_{des} \sin \psi_T + \theta_{des} \cos \psi_T)g$$

$$\ddot{w}_{2,des} = (-\phi_{des} \cos \psi_T + \theta_{des} \sin \psi_T)g \qquad (16)$$

$$\ddot{w}_{3,des} = \frac{u_{1,des}}{m}$$

Utilization of the presented above dependencies allows to provide the setpoints of the pitch and roll angles for the needs of the quadrotor orientation control (10) (15). The value of force setpoint $u_{1,des}$ is determined in the following way:

$$\phi_{des} = (\ddot{w}_{1,des} \sin \psi_T - \ddot{w}_{2,des} \cos \psi_T) / g$$

$$\theta_{des} = (\ddot{w}_{1,des} \cos \psi_T + \ddot{w}_{2,des} \sin \psi_T) / g \qquad (17)$$

$$u_{1,des} = m\ddot{w}_{3,des}$$

To determine the flight path in the 3D space, a method from involving determination of the nearest point of the trajectory w_T for the current position w is utilized. Position and velocity errors are defined respectively:

$$e_p = w_T - w$$

$$e_v = \dot{w}_T - \dot{w} \qquad (18)$$

The calculation of the desired acceleration $\ddot{w}_{i,des}$ is carried out in the PD controller feedback loop in following way:

$$\ddot{w}_{i,zad} = k_{p,i}e_{i,p} + k_{d,i}e_{i,v} \qquad (19)$$

Ultimately, using equation (19) it is possible to determine desired values of roll and pitch angles and $u_{1,des}$ according to equation (17).

2.5. Obstacle avoidance controller

Quadrotor control system has two independent feedback control loops (Fig. 2). The inner control loop is responsible for quadrotor stabilization, while the outer loop is associated with the UAV position control. The inner loop uses the data read from the three axis accelerometer and gyroscope for the control of the roll, pitch and yaw angles (ϕ, θ, ψ). This loop works with 200 Hz frequency. On the other hand the outer loop, utilizes the quadrotor GPS position and GPS velocity data to control the flight.
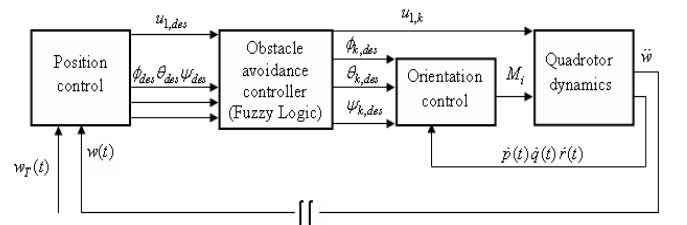

Fig. 2. A block diagram of the quadrotor control system

The obstacle avoidance system includes an additional block (fuzzy logic controller) in the inner loop. This block is responsible for producing the corrections k_φ, k_θ to the desired values of navigational angles (φ_{des}, θ_{des}). These adjustments are described in the following way:

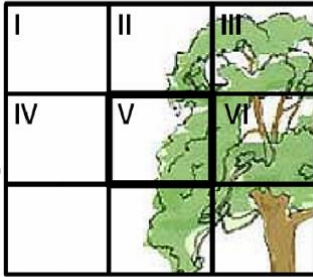$\phi_{k,des} = \phi_{des} \pm k_\phi$ – correction of the desired rolling angle,

$\theta_{k,des} = \theta_{des} \pm k_\theta$ – correction of the desired pitching angle.

Corrections k_T to the throttle signal are calculated with following simplified formula:

$$k_T = 30\% \cdot u_{1,des} \tag{20}$$
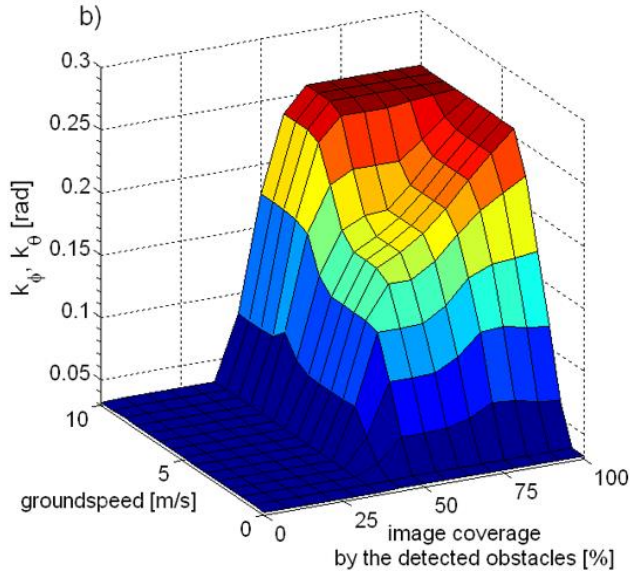
$$u_{1,k} = u_{1,des} + k_T \tag{21}$$

a)

b)

Fig. 3. Obstacle detection a) Image sections definition,
b) sample fuzzy logic control surface

Signal of desired throttle is calculated as follows:

Image obtained by the vision system can be shown schematically in Fig. 3a. Whole image is divided to 6 main sections. Camera is oriented always in flight direction of the quadrotor. Vision algorithm analyze only the center of the image (section V on the Fig.3a). Fig.3b represents surface whereby corrections k_φ, k_θ are calculated. Control signal is produced basing on vehicle ground speed and coverage of the section V (center of the analyzed image) by the detected obstacle.

Detection of obstacle in the section V of the image, starts collision avoidance procedure and next, sequent image sections are analyzed and processed. The correction values k_φ, k_θ, k_T are determined based on information from analyzed sequent image sections. In the situation when the obstacle free space is detected in the IV and VI sections (Fig. 3a), the correction k_ϕ with the sign appropriate to the maneuver direction is produced according to modeled control surface (Fig. 3b). For image sections I and III, k_T is determined with (20) and also appropriately signed k_ϕ is pro-

duced with control surface from Fig. 3b also. In the case of section II the correction k_T is overwritten only. The last possibility is when in the whole image is no obstacle free space. In this case, correction k_T is obtained with equation (20) and k_θ is calculated in following manner:

$$\theta_{des} \pm k_\theta \approx 0 \tag{22}$$

what causes a vertical ascent of the UAV. The vertical ascent is continuing until the obstacle free space is localized in the image. Above procedures and control rules have good performance in the open space and during outdoor flights. In the case of indoor flights it is needed to use additional correction to yaw angle desired value ψ_{des}.

3. SIMULATION RESULTS

Basing on equations (7) the simulation model of the quadrotor was build in Matlab/Simulink software with the usage of specialized toolboxes like Control System, Flight Dynamics and Control, Aerospace and Fuzzy Logic. The aim of the simulation research was a preliminary selection of the parameters that are used in the autonomous mission control system of the unmanned aerial vehicle. Dynamically changing simulation environment has been programmed as the model of the virtual reality written in VRML (Virtual Reality Modelling Language). Virtual simulation world reproduces the area in which the in-flight tests were to be conducted. This will allow the comparison of the results obtained from the simulation with the measurements taken directly from the conducted experiment. The simplified model of image processing methods was approved in the simulation tests. Brightness control system described in Cieśluk and Gosiewski (2013, 2014), that is essential during in-flight tests, wasn't used during simulation studies. Whereas the law of UAV position control, autopilot operating modes and the area describing the obstacles were modeled. Image used by the obstacle avoidance algorithm is continuously extracted from a moving quadrotor in 3D space. During simulation tests image refresh rate is set at 10 fps. The flight simulation screen is presented in Fig. 4. The graphs show the currently generated flight path and the result of vision obstacle detection algorithm.
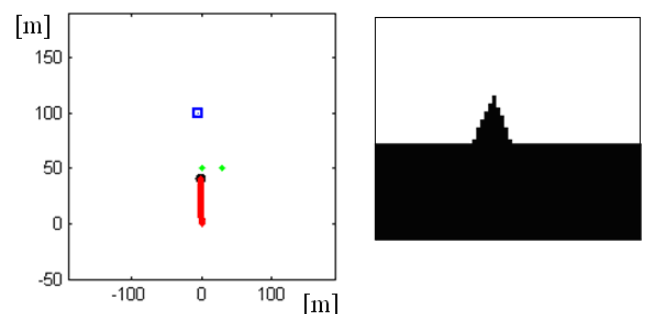

Fig. 4. Simulation studies application (UAV flight path - left side, output of the obstacle detection algorithm (processed image) - right side)

Simulation study was conducted for the model which reflects the area of out-door field tests. Fig. 5 presents the pictures taken during the proving ground studies.

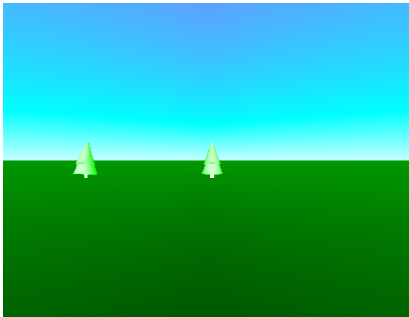Jakub Cieśluk, Zdzisław Gosiewski, Leszek Ambroziak, Sławomir Romaniuk
Computationaly Simple Obstacle Avoidance Control Law for Small Unmanned Aerial Vehicles

DOI 10.1515/ama-2015-0010

The influence of changes in the sequence of the image controlled areas to the direction of the maneuver is presented in Fig. 7. Edges of the map show the position expressed in meters. Green points represents the obstacles, while the blue square is the quadrotor destination waypoint. Analogously the red thick line shows the travelled path. Example shows that the direction of the maneuver is highly dependent on the established criteria for image search of obstacle-free sections. During simulation tests, different forms of the control surface were tested. Results for different types of the control surfaces are presented in the Fig. 8. In simulation research the best possible shape of the control surface was chosen, taking into account quadrotor reaction aggressiveness.

4. IN-FLIGHT TESTS

The most important step in an obstacle avoidance controller synthesis is in-flight testing. At the same time, it is the most risky part of the research. The study has been carried out on the airfield. Own build quadrotor airframe with ArdupilotMega 2.0 was used as a testing object. ArdupilotMega 2.0 runs custom control application. The image processing algorithms are implemented on a small, smart camera with auto iris lens (Cieśluk and Gosiewski, 2014) and mass of 220g. Image processing algorithm was working with 42 Hz frequency.

Fig. 5. View of the airfield

Fig. 6. Field area modeled in the VRML
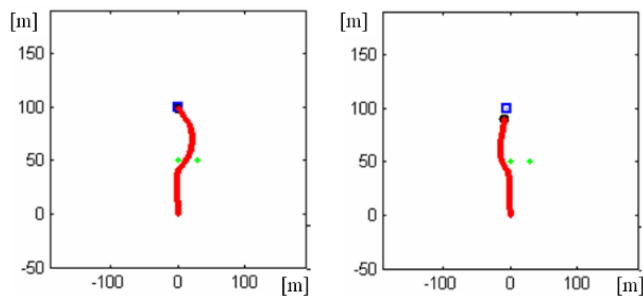(Virtual Reality Modelling Language)

Fig. 7. Different quadrotor reactions depending
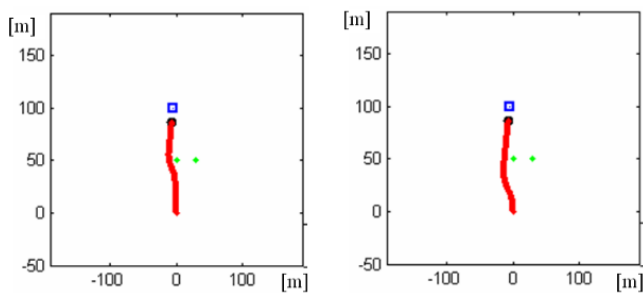on image search algorithm configuration

Fig. 8. Quadrotor flight paths for different control surfaces

Fig. 9. Field experiments: a) picture from the webserver of vision system
b) photo of the tree as an obstacle (made during the field test)

The quadrotor was also equipped with a wireless WiFi router (90g) and LiPo battery 4600mAh. Total mass of all components was less than 400g. Trajectory was planned to meet on its way at least one obstacle. Tests were carried out for short range missions to keep constant radio contact with the quadrotor. The Fig. 9 presents quadrotor during in-flight tests and the vision system webserver.

In the Fig.10 quadrotor flight paths obtained during in-flight tests are presented. Flight paths are marked with dark blue lines on the airfield satellite view from ground control station. Preselected flight paths should be straight, but in case of obstacle vision system acting, desired path was corrected to amount of obstacle appearance.

Fig. 10. Quadrotor flight paths during in-flight tests (based on the satellite maps of the investigated area)

5. CONCLUSIONS AND FUTURE WORK

Proposed vision obstacle controller connected with fuzzy logic technique to control surface modeling is an effective method of controlling small UAVs autonomously. Obtained during simulation studies and in-flight tests results indicate that vision obstacle avoidance system can be used in the real applications but we have to take into account that experimental tests were properly arranged (straight path line with one, clear, explicit obstacle). It will be much more difficult to use this system and algorithm in the dynamic environment, bad weather conditions and to small obstacles. Several unsuccessful attempts were recorded, however taking them as the base it is hard to say, whether the obstacle detection system was guilty of the failure.

Further works will be strictly associated with the operation effectiveness improvement of the obstacle detection methods pre-

sented in the work. Consecutive tests will be conducted for more complex missions.

REFERENCES

1. **Bresciani T.** (2008), *Modelling, Identification and Control of a Quadrotor Helicopter*, Master's thesis, Lund University, Sweden.
2. **Cieśluk J., Gosiewski Z.** (2012), Vision sky detection system used to obstacle avoidance by unmanned aerial, Mechanics in Aviation XV, 2012, pp. 509-523.
3. **Cieśluk J., Gosiewski Z.** (2013), A Stereovision System for Real Time Obstacle Avoidance by Unmanned Aerial Vehicle, *Solid State Phenomena*, Vol 198, pp. 159-164.
4. **Cieśluk J., Gosiewski Z.** (2014), Image brightness control method used for obstacles avoidance by unmanned aerial vehicle, *Mechanics in Aviation*, 16, 2014, 279-290.

5. **Guzel M. S., Bicker R.** (2011), *Vision Based Obstacle Avoidance Techniques, Recent Advances in Mobile Robotics*, Dr. AndonTopalov (Ed.), InTech, UK, 83-101.

6. **Herisse B., Russotto, F.-X., Hamel, T., Mahony, R.** (2008), Hovering flight and vertical landing control of a VTOL Unmanned Aerial Vehicle using Optical Flow, *IEEE International Conference on Intelligent Robots and Systems*,pp. 801 – 806.

7. **Hoffmann G. M., Huang H., Waslander S. L, Tomlin C. J.** (2011), Precision flight control for a multi-vehicle quadrotor helicopter testbed, *Control Engineering Practice*, Vol. 19, 1023–1036.

8. **Khatib O.** (1985), The Potential Field Approach and Operational Space Formulation in Robot Control, *Proc. Fourth Yale Workshop on Applications of Adaptive Systems Theory*, Yale University, New Haven, Connecticut, 208-214.

9. **Kownacki C.** (2013), Successful Application of Miniature Laser Rangefinders in Obstacle Avoidance Method for Fixed Wing MAV, *International Journal of Robotics and Automation*, 10.2316/ Journal.206.2013.3.206-3936.

10. **Meier L., Tanskanen P., Heng L., Lee G. H., Fraundorfer F., Pollefeys M.** (2012), PIXHAWK: A micro aerial vehicle design for autonomous flight using onboard computer vision, *Autonomous Robots*, 33 (1-2), 21-39.

11. **Mellinger D., Michael N., Kumar K.** (2012), Trajectory generation and control for precise aggressive maneuvers with quadrotors, *The International Journal of Robotics Research*, Vol. 31, No. 5, 664-674.

12. **Modi S. B., Chandak P., Murty V. S., Hall E. L**. (2001), Comparison of three obstacle-avoidance methods for a mobile robot, *Proc. SPIE 4572, Intelligent Robots and Computer Vision XX: Algorithms, Techniques, and Active Vision*, pp. 290-297.

13. **Sabatini R., Gardi A., Richardson M. A.** (2014), LIDAR Obstacle Warning and Avoidance System for Unmanned Aircraft, *International Journal of Mechanical, Aerospace, Industrial and Mechatronics Engineering*, Vol. 8, No 4, 702-713.

14. **Shojaeipour S.** (2010), Webcam-based mobile robot path planning using Voronoi diagrams and image processing, *Proceedings of the 9th WSEAS international conference on Applications of electrical engineering*, World Scientific and Engineering Academy and Society (WSEAS), Penang, Malaysia, 151-156.

15. **Soumare S., Ohya A., Yuta S.** (2002), Real-Time Obstacle Avoidance by an Autonomous Mobile Robot using an Active Vision Sensor and a Vertically Emitted Laser Slit, *Intelligent Autonomous Systems*, 7, 301-308.

16. **Wang L.** (2001), Continuous time model predictive control design using orthonormal functions, *International Journal of Control*, Vol. 74(16), 1588-1600.